Am J Transl Res 2026;18(6):5064-5081
www.ajtr.org /ISSN:1943-8141/AJTR0171000

Original Article

Injury thresholds and early-warning biomarkers for horizontal acceleration induced cervical damage in New Zealand rabbits

Yong-Cheng Liang, Shen-Hui Yin, Er-Gang Zhao, Yan-Bin Zhan, Wei Wang

Naval Medical Center of The People's Liberation Army, Navy Medical University, Shanghai 200082, The People's Republic of China

Received December 24, 2025; Accepted May 7, 2026; Epub June 15, 2026; Published June 30, 2026

Abstract: Cervical injury is a common occupational health concern among pilots. At present, most studies in this area concentrate on post-injury diagnosis or retrospective analysis of high-risk exposure factors. In contrast, research on candidate early warning biomarkers remains limited. To address this gap, we employed New Zealand rabbits as an experimental model to investigate cervical spine injuries induced by horizontal acceleration under conditions relevant to pilots. By integrating approaches of imaging, histopathological evaluation, and multi-omics profiling, we determined the injury thresholds for single impact and cumulative exposure to the cervical spine. Furthermore, the potential biomarkers for candidate early cervical injury warning were identified. The study demonstrated that a single impact of -5Gx could cause acute injury to the trapezius muscle, while a single impact of -9Gx could lead to acute intervertebral disc injury in New Zealand rabbits. Additionally, cumulative exposure to -6Gx over 3 weeks could induce degenerative changes in the cervical intervertebral discs. Furthermore, this research identified four serum-based and five intervertebral disc-derived biomarkers associated with early-stage injury. This study provides theoretical support for the injury thresholds for cervical damage among pilots and proposes candidate biomarkers for pre-injury early warning systems.

Keywords: Horizontal acceleration, cervical injuries, injury thresholds, warning biomarkers

Introduction

Cervical injuries can cause serious occupational health challenges among high-performance fighter pilots [1]. During typical mission profiles such as aerial combat and arrested landing, the cervical spines of pilots are subjected to repeatedly high-magnitude, short-duration, and multi-directional acceleration loads. Among these, horizontal acceleration, especially in the -Gx direction, is a key mechanical factor inducing acute and chronic cervical injuries [2]. Epidemiological evidence shows that these injuries are not only highly prevalent and recurrent, but can also lead to chronic pain, cervical degenerative changes, and even neurological dysfunction in severe cases. As a result, these injuries pose a significant threat to flight safety and may hinder the long-term career development of pilots [3].

Current research on cervical injuries in pilots have mainly focused on retrospective analyses, including clinical diagnoses [4], treatment outcomes [5], and post-injury risk factors [6]. While informative, existing research remains fundamentally reactive in nature, offering little insight into early warning signs or prospective risk assessment before damage occurs [7]. More critically, systematic and quantitative data on the response of cervical tissues to horizontal acceleration remain strikingly scarce, particularly under conditions of cumulative low-intensity exposure. This knowledge gap weakens the biomechanical and pathophysiological basis underlying current protective standards and equipment designs, thereby hindering the shift from passive treatment to proactive prevention. Clarifying the mechanical thresholds [8] and molecular warning signals [9] associated with acceleration-induced cervical injury has thus emerged as a pressing priority for both aviation medicine and protective engineering. This study was designed to address these needs by establishing a well-controlled animal model, precisely

https://doi.org/10.62347/QATP7456

quantifying the biomechanical limits of cervical injury and identifying biomarkers suitable for early risk detection.

New Zealand rabbits were selected as the experimental model because their cervical spine exhibits biomechanical properties highly similar to those of humans [10]. The study was designed around two main components. First, a custom-designed horizontal impact device, developed based on equivalent mechanics principles, was used to simulate a single rapid deceleration event, thereby establishing the acute injury threshold for both the trapezius muscle and cervical intervertebral discs. Second, a four-arm animal centrifuge was applied to model repeated acceleration exposure [11], allowing the investigations of the cumulative injury thresholds and the temporal progression of intervertebral disc degeneration. To overcome the limitations of conventional morphological assessment alone, this work integrated multiple analytical techniques, including magnetic resonance imaging, histopathological staining and proteomic profiling [12]. By systematically analyzing serum and intervertebral disc tissue, this study sought to identify early-warning biomarkers indicative of incipient pathological changes prior to the onset of overt structural damage. Subsequent bioinformatics analysis was further performed to clarify the underlying pathophysiological mechanisms associated with these molecular markers.

Taken together, this study established a quantitative threshold reference and an early-warning tool for the prevention of pilots' cervical injuries. Furthermore, it offered a novel perspective on the universal mechanism of mechanical stress-induced soft tissue degeneration.

Materials and methods

The experimental device that simulates a single impact of horizontal acceleration in New Zealand rabbits

The device for simulating acceleration in animal experiments is based on the principle of equivalent mechanics.

According to Newton's second law:

$F = ma$, (1)

The acceleration can be defined as the force acting on the object divided by its mass. A fundamental physical quantity related to acceleration is gravity, denoted as g (Earth's gravitational constant), which represents the acceleration produced by Earth's gravitational field. Near the surface of the Earth, an object in free fall undergoes an acceleration of approximately 9.8 m/s^2. For practical and intuitive purposes, acceleration in biomechanical and experimental studies is commonly expressed in units of g. Put simply, an acceleration of ng corresponds to a force equivalent to n times the object's weight, as described by the relation $F = nmg$, where mg is the gravitational force acting on the object. This principle forms the basis of equivalent mechanics: with the known gravitational force, we can simulate a desired acceleration in experimental settings in a controlled and quantifiable way.

Based on the principle of equivalent mechanics, we designed and constructed a device to simulate acceleration for animal experiments (Figure S1A). Representative CAD drawing is shown in Figure S1B. This device must fulfill three basic requirements. First, it should securely immobilize New Zealand rabbits in a vertical posture. Second, it must be capable of applying a horizontal force to the head and cervical of New Zealand rabbits. Third, the magnitude of this horizontal force should be adjustable. The trunk vest within the experimental device can securely immobilize the rabbit on the experimental platform; additionally, an adjustable counterweight module ensures that its weight corresponds to n times of the rabbit's head. The pulley conversion module can redirect the counterweight module into a horizontal leftward pulling force; furthermore, a cervical brace can serve as a point of applying this pulling force directly onto the animal's cervical spine (Figure S1A).

The experimental device mainly simulates the force exerted on the animal's cervical spine during sudden deceleration, where the trunk is restrained while the head is allowed to move freely. According to the principle of equivalent mechanics, under hypothetical operating conditions, the force acting on the cervical spine of an animal corresponds to n times the weight of its head. When simulating a working condition of -5Gx, the force on the rabbit's cervical spine

is about five times the gravitational weight of its head.

Calculating the head weight of New Zealand rabbits

To simulate acceleration using animal experimental equipment, it is necessary to measure the weight of the New Zealand rabbit's head in advance and adjust the weight of the counterweight module accordingly. During the pre-experiment sampling, three New Zealand rabbits were anesthetized and euthanized using pentobarbital sodium. Their body weights were measured. Next, their heads were dissected along the inferior border of the mandible and occipital bone and the weight of each head was measured individually, with the detailed results presented in Table S1.

A mathematical model describing the relationship between the body weight and head weight of rabbits was established using Excel, expressed by the equation $y=0.0783x$, $R^2=0.8402$ (Figure S1C). This indicates that the weight of a rabbit's head is approximately equal to the weight of the rabbit body times 0.0783. In subsequent formal experiments, this coefficient will be employed to calculate the head weight based on measured body weights [13].

Cervical -Gx over limit overload exposure experiment

This experiment was approved by the Animal Experiment Science and Technology Ethics Committee of the Air Force Medical University of the Chinese People's Liberation Army, with approval number 20250016. A total of 21 healthy 6-month-old New Zealand rabbits weighing 2.4-3.5 kg were randomly assigned to 7 groups (n=3 per group). Rabbits in the control group were only fixed with a trunk vest and received no additional intervention. The remaining 18 rabbits in the experimental groups were similarly fixed and exposed to -Gx directional impact loading, starting at -5Gx with a peak duration of < 2 s. The acceleration magnitude was incrementally increased by 2Gx per group, up to a maximum of -15Gx (Table S2). This loading protocol simulated inertial loading on the cervical spine during sudden deceleration, in which the trunk was fixed while the head moved freely, generating an inertial force equivalent to n-fold gravitational force.

Following exposure, New Zealand rabbits were anesthetized for cervical MRI scanning. The rabbits were then euthanized via anesthetic overdose and placed in the prone position. After posterior cervical skin incision and blunt dissection, bilateral trapezius muscles were harvested and fixed in 4% paraformaldehyde. C4-C5 vertebral segments were isolated following removal of adjacent soft tissues, and similarly fixed in 4% paraformaldehyde. Muscle specimens were directly processed for paraffin embedding, sectioning, and hematoxylin-eosin (HE) staining, while vertebral samples were decalcified before the same histological procedures. Morphological alterations were subsequently evaluated.

Cervical injury caused by cumulative overload

A four arm multi degree of freedom animal centrifugation from the Air Force Medical University was used to simulate the acceleration environment. The radius of the animal centrifugation is 2 m, and it can simulate - Gx range from -1 to -16Gx (Figure S2A). Schematic of the centrifugation system was shown in Figure S2B.

A custom fixation and restraint device for New Zealand rabbits was designed and manufactured via 3D printing to secure animals during centrifugation. To protect experimental animals, self-adhesive cushion foam was applied to areas of the restraint box subject to friction (Figure S2C).

The protocol for cumulative overload exposure

This experiment was approved by the Animal Experiment Science and Technology Ethics Committee of the Chinese People's Liberation Army Air Force Medical University, with approval number 20250016. A total of 64 New Zealand rabbits were randomly divided into four centrifugation groups (1, 2, 3, and 4 weeks) and four corresponding time-matched control groups (n=8 per group). Animals in the experimental groups were subjected to daily -6Gx centrifugation at a ramp rate of 1 G/s, consisting of five 1-minute exposures with 5-minute interval between sessions (Figure S2D). Centrifugation was performed until the scheduled duration was completed. Control rabbits were housed under identical conditions without exposure.

After the exposure, blood samples were collected first to minimize anesthesia-related mortality. After precordial hair removal, the apex beat was identified at the left 2nd-3rd intercostal space, followed by disinfected with 75% alcohol. A 5 ml fine needle syringe was inserted at a 45° angle toward the right and inferior direction to a depth of 1.5-2 cm. Correct placement was confirmed by needle oscillation with the heartbeat. After slowly drawing 5 mL of blood under low negative pressure, the needle was withdrawn, and the puncture site was disinfected. The blood was placed in a serum separation tube. The supernatant was then transferred into a 1.5 ml EP tube and stored at -80°C for subsequent proteomic analysis.

Following blood collection, all rabbits were anesthetized for cervical MRI analysis. Upon completion of imaging, the animals were euthanized via anesthetic overdose and positioned prone. After posterior cervical skin incision, bilateral trapezius muscles were bluntly dissected. The left muscle was harvested and fixed in 4% paraformaldehyde, while the right muscle was rinsed with PBS, blotted dry, and stored at -80°C for further analysis.

The C2-C7 cervical vertebrae were then excised with surrounding soft tissues removed. The C4-C5 segment was isolated and fixed in 4% paraformaldehyde, whereas C2-C3, C3-C4, and C5-C6 intervertebral discs were collected and frozen for omics assays. Muscle specimens were directly processed for paraffin embedding, sectioning, and hematoxylin-eosin (HE) staining; vertebral samples were decalcified before undergoing identical histological processing for morphological evaluation.

Results

Injury thresholds for trapezius muscle and cervical intervertebral discs to single horizontal acceleration in New Zealand rabbits

To investigate the injury thresholds of New Zealand rabbits response to single horizontal acceleration, six groups (n=18) were exposed to incremental -Gx impacts ranging from -5Gx to -15Gx. MRI analysis showed no obvious injury on intervertebral disc or trapezius muscle (**Figure 1A**). However, HE staining showed muscle fiber necrosis and hemorrhage in the trapezius muscle after a single -5Gx horizontal impact. In the higher G-value groups, inflammatory cell infiltration was also observed. Nevertheless, no discernible trend of worsening injury severity with increasing G-values was observed (**Figure 1B**). Furthermore, HE staining revealed reduced intervertebral disc height and the formation of nucleus pulposus fissures in vertebral bodies after a single -9Gx horizontal impact. Moreover, progressively severe structural damage, including annular fibrosus tears, was observed with increasing G-values (**Figure 1C**). Taken together, these results indicated that the injury threshold response to single horizontal acceleration for the trapezius muscle in New Zealand rabbits is -5Gx or less, whereas that for the intervertebral discs is -9Gx.

Injury thresholds to cumulative horizontal acceleration in New Zealand rabbits

To investigate the injury thresholds response to cumulative horizontal acceleration, New Zealand rabbits were exposed to -6Gx acceleration for various duration using an animal centrifuge.

In the MRI images of the corresponding control group, the nucleus pulposus exhibited uniform high signal intensity, while the annulus fibrosus appeared as a low-signal ring surrounding the bright nucleus pulposus. The vertebral bodies displayed moderately high signal intensity, appearing brighter than the annulus fibrosus but darker than the nucleus pulposus or cerebrospinal fluid, with relatively uniform signal distribution. The trapezius muscle showed intermediate to low signal intensity, with homogeneous signal and distinct muscle fiber texture. While in the MRI images of the 1 and 2-week centrifugation group, herniation of the cervical disc was observed, compressing the cerebrospinal fluid band dorsally in the New Zealand rabbits. Decreased T2 signal intensity was observed in the intervertebral discs of the 3 and 4-week centrifugation group, indicating intervertebral disc degeneration (**Figure 2A**). These results suggested that centrifugation-induced acceleration in the -Gx direction promotes posterior compression of the intervertebral disc by adjacent vertebral bodies, leading to disc herniation. Furthermore, this loading conditions increased stress on the disc, and degenerative changes likely occurred once the cumulative mechanical load exceeded a critical threshold.

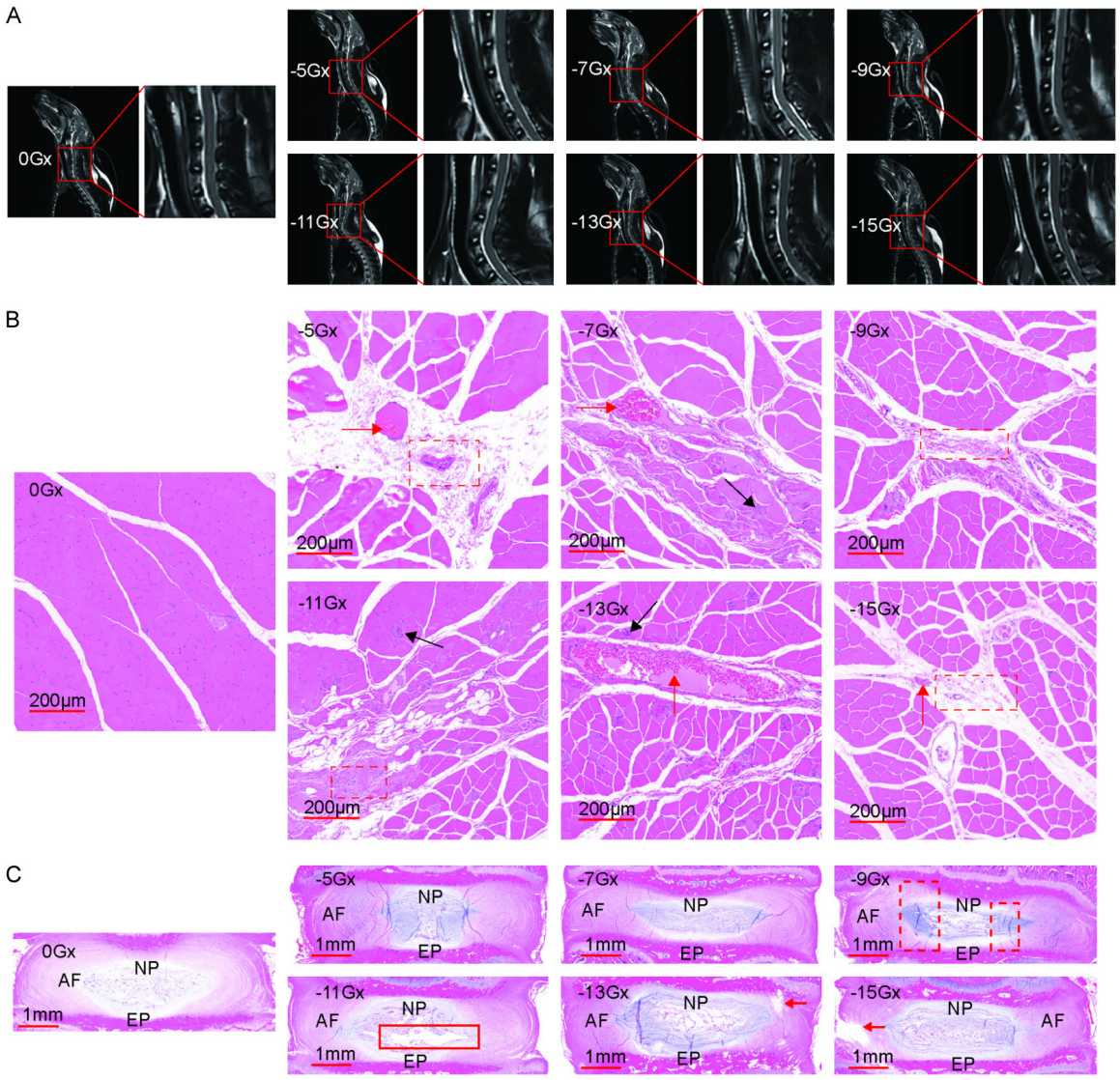

Figure 1. The impact of horizontal acceleration on the cervical vertebrae. A. Representative MRI images of the cervical of New Zealand rabbits, T2, sagittal. No evidence of decreased T2 signal in the nucleus pulposus or disc protrusion was found; B. Representative HE staining of the cervical trapezius muscle of New Zealand rabbits. Objective, 5×. Scale bars, 200 μm. Dashed red box indicated muscle fiber necrosis. Red arrow indicated hemorrhage. Black arrow indicated inflammatory cell infiltration; C. Representative HE staining of the cervical 4/5 intervertebral disc in New Zealand rabbit, Objective, 2×. Scale bars, 1 mm. Dashed red box indicated a reduction in the intervertebral disc height. Solid red box indicated the nucleus pulposus fissures. Red arrow indicated the annulus fibrous tears. The leftmost side of each subgraph is the 0Gx control group. At the upper section, the groups are arranged from left to right as follows: -5Gx, -7Gx, and -9Gx. At the lower section, the groups are organized from left to right in this order: -11Gx, -13Gx, and -15Gx. Sample size (n=21).

HE staining of the trapezius muscle in New Zealand rabbits revealed no evidence of muscle damage in either the centrifugation group or the control group (**Figure 2B**). Although an initial single impact of -5Gx could cause injury to the trapezius muscle, the lack of detectable damage under long-term cumulative exposure to -6Gx may be attributed to muscular adaptation to this intensity of mechanical loading or effective repair of daily stress-induced microtrauma [14].

In control groups, the cervical vertebral bodies exhibited intact structure, characterized by normal cellular morphology, clear and regular concentric lamellae within the annulus fibrosus

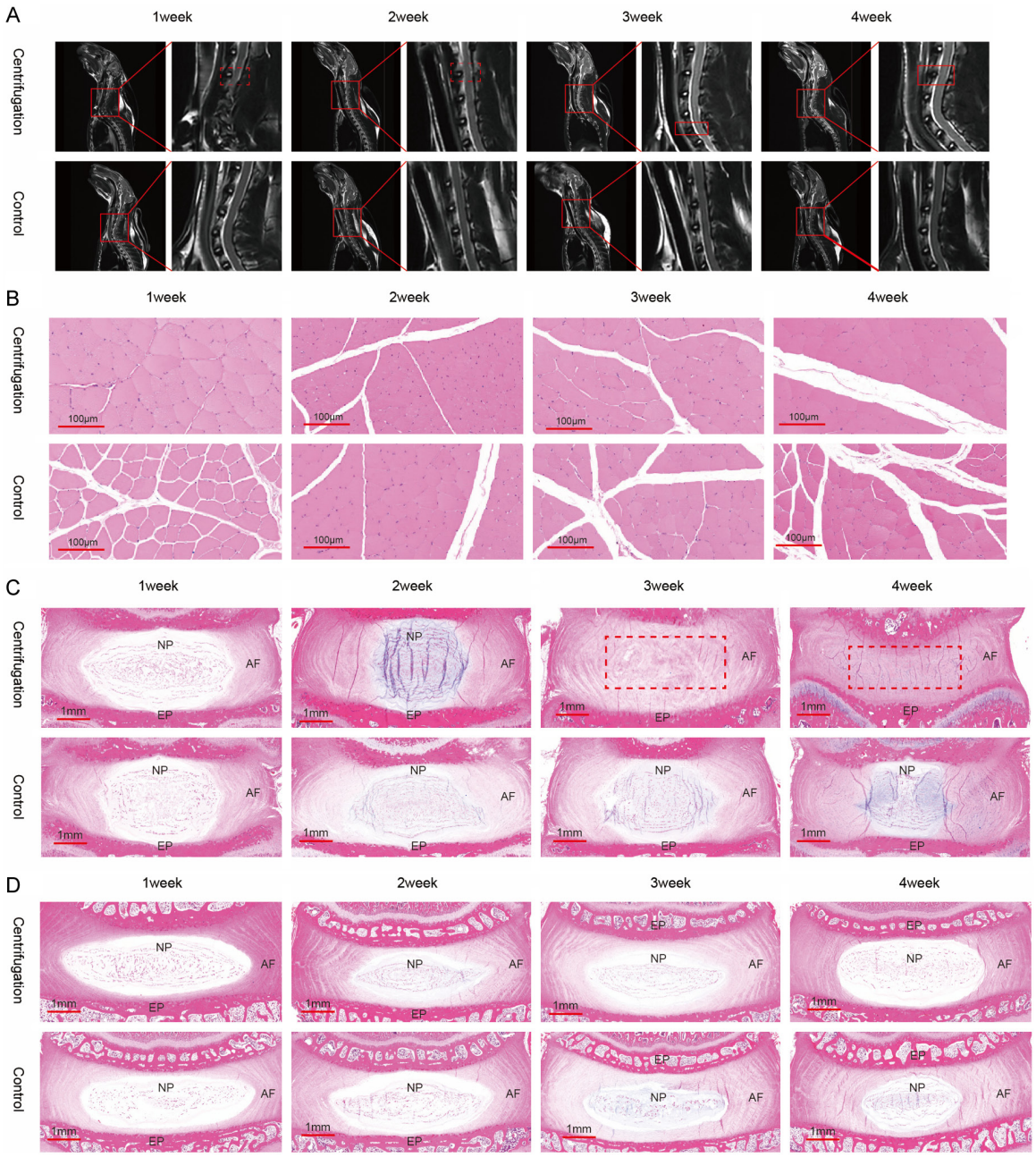

Figure 2. Images and morphological results of cumulative overload injury. A. Representative MRI images of the cervical of New Zealand rabbits, T2, sagittal. Red dashed boxes indicated intervertebral disc protrusion compressing the CSF space, and red solid boxes indicated decreased T2 signal intensity of the nucleus pulposus; B. Representative HE staining of the cervical trapezius muscle of New Zealand rabbits. Objective, 5×. Scale bars, 100 μm; C. Representative HE staining of the cervical 4/5 intervertebral discs in New Zealand rabbits. Objective, 2×. Scale bars, 1 mm. Dashed red box indicated fibrosis of the nucleus pulposus; D. Representative HE staining of the lumbar 4/5 intervertebral discs in New Zealand rabbits. Objective, 2×. Scale bars, 1 mm. The upper section of each subgraph represents the centrifugation group, and the lower section represents the control group. From left to right, these groups correspond to 1-week group, 2-week group, 3-week group, and 4-week group, respectively. Sample size (n=64).

and clearly delineated boundaries of each component, and with no signs of degeneration or injury. We found that in the 1 and 2-week centrifugation groups, both the nucleus pulposus and annulus fibrosus displayed normal morphological features. From 3 weeks of centrifuga-

tion, fibrosis of the nucleus pulposus was observed, suggesting the onset of intervertebral disc degeneration (**Figure 2C**). This result indicated that intervertebral disc degeneration occurred once the cumulative mechanical loading exceeded a specific threshold. Furthermore, HE staining of rabbit lumbar spine segments (L4-L5) revealed no signs of injury to vertebral bodies and intervertebral discs in either the centrifugation group or control group (**Figure 2D**). This absence of structural damage likely resulted from the secure immobilization of the lumbar region throughout the experiment. Collectively, these findings indicated that the interval between 2-3 weeks represented a critical threshold for cumulative damage induced by horizontal acceleration.

Candidate early warning and injury indicators in serum proteomics of New Zealand rabbits

To identify the potential warning markers for cervical injury, serum samples from both experimental groups and control groups were collected and subjected to proteomic analysis. PCA was performed on 32 samples, reducing multiple protein expression variables from high dimensions to a few independent variables. The first two principal components (PC) explained 33.3% of the total variation, with principal component 1 (PC1) accounting for 23.5% and principal component 2 (PC2) accounting for 9.8%. The results showed significant differences between sample groups and clear group separation (**Figure 3A**). We analyzed differentially expressed proteins in the centrifugation group compared with the corresponding control group and determined their intersection. We found that the expression level of A0A5F9CQH5 was upregulated at 1, 2, 3 and 4 weeks, while the expression of PSMA8, GPX6, and CAT proteins were upregulated at 2, 3 and 4 weeks in the centrifugation group (**Figure 3B**). These four markers showed consistent changes both before and after the injury became apparent, positioning them as promising candidates for early warning.

Nucleus pulposus cells rely on a proteoglycan- and collagen-rich extracellular matrix for survival and function. Mechanical loading frequently disrupts the delicate balance between matrix synthesis and catabolism [15]. In our proteomic analysis, we identified A0A5F9CQH5, also known as Complement C1q tumor necrosis factor-related protein 3 (C1QTNF3), is a member of the CTRP family. This protein regulates energy metabolism, inflammation, and matrix homeostasis. Studies have shown that C1QTNF3 promotes proteoglycans and collagen synthesis in chondrocytes while suppressing their degradation, partly via activation of the AKT signaling pathways [16]. In our model, the upregulation of C1QTNF3 under cumulative mechanical loading may represent a compensatory cellular response that helps maintain extracellular matrix homeostasis and alleviate injury caused by mechanical stress.

The microenvironment of intervertebral disc cells is defined by hypoxia, nutrient deprivation, and sustained mechanical strain. These factors collectively promote the accumulation of misfolded and damaged proteins, triggering endoplasmic reticulum stress and ultimately apoptosis [17]. As a subunit of the 20S proteasome PSMA8 is essential in the ubiquitin-proteasome system. In our model, repeated mechanical loading exacerbated the accumulation of damaged proteins. Cells responded by upregulated PSMA8 to enhance waste clearance and sustain viability. When the proteasome system becomes overwhelmed, however, proteotoxic stress develops, accelerating cell death and promoting intervertebral disc degeneration. Thus, PSMA8 may serve as a sensitive marker of cellular stress under mechanical loading.

Oxidative stress is a key driver of intervertebral disc degeneration. Mechanical loading and inflammation can trigger reactive oxygen species (ROS) generation, inducing oxidative damage to lipids, proteins. This further compromises cellular function, promotes matrix-degrading enzyme release, and accelerates cellular senescence and apoptosis [18]. As an antioxidant enzyme, GPX6 (Glutathione Peroxidase 6) detoxifies hydrogen peroxide and organic peroxides, protecting cells against oxidative injury. In our model, cumulative mechanical exposure triggered substantial ROS production, and the upregulation of GPX6 likely reflects an adaptive antioxidant response. Similarly, CAT (Catalase) also participates in hydrogen peroxide decomposition into water and oxygen, thus maintaining redox balance. Its upregulation further supported the activation of endogenous antioxidant defenses under sustained mechanical

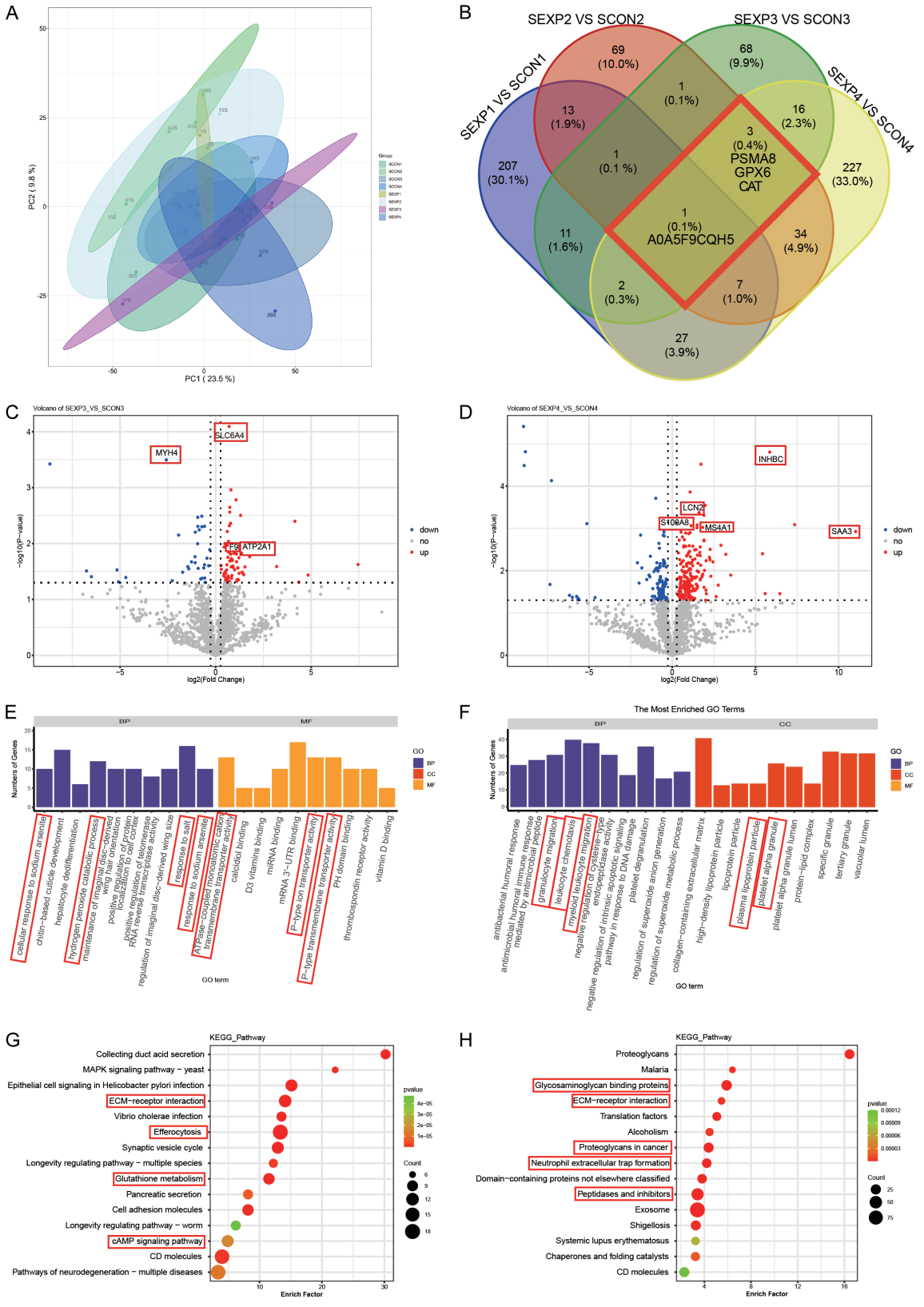

Figure 3. Proteomic analysis of serum samples. A. Principal Component Analysis of proteins in experimental groups and control groups; B. Venn Differences and Similarities analysis of proteins in experimental groups and control groups, sample size (n=64); C. Volcano plot analysis of differentially expressed proteins in the three-week experi-

mental group compared with the 3-week control group; D. Volcano plot analysis of differentially expressed proteins in the 4-week experimental group compared with the 4-week control group; E. GO analysis of differentially expressed proteins in the 3-week experimental group compared with the 3-week control group; F. GO analysis of differentially expressed proteins in the 4-week experimental group compared with the 4-week control group; G. KEGG analysis of differentially expressed proteins in the 3-week experimental group compared with the 3-week control group; H. KEGG analysis of differentially expressed proteins in the 4-week experimental group compared with the 4-week control group.

stress. Consistent with previous reports showing disrupted antioxidant enzyme expression in degenerative intervertebral disc tissue [19], the coordinated upregulation of CAT and GPX6 in our study confirmed the induction of oxidative stress by mechanical loading.

Taken together, we identified A0A5F9CQH5, PSMA8, GPX6, and CAT in serum as potential warning markers for cervical injuries in pilots undergoing cumulative horizontal acceleration training.

Histological analysis revealed intervertebral disc injuries in 3- and 4-week centrifugation groups. To identify associated injury biomarkers, we further analyzed differentially expressed proteins between these time-matched centrifugation groups and control groups. The top 10 upregulated and 10 downregulated proteins after 3-week centrifugation included TCHH, MYH4, HDGF, APOD, EBP41L2, RDX, MYH1, CTSV, SBSN, GPNMB, SLC6A4, ATP6V1E1, CAT, RAB10, RPS15A, GP9, CSPEP1, F9, ATP2A1, and TRPC6 (**Figure 3C**). MYH1 and MYH4 are myosin heavy chains. MYH4 is a marker of fast contraction, and fatigue-prone type IIB muscle fiber. Their downregulation in the 3-week centrifugation group reflected mechanical stress, overuse, and possible muscle fiber-type switching. Muscle fatigue may promote inflammatory factors release, aggravating local pain and tissue degeneration [20]. ATP2A1, a sarcoplasmic/endoplasmic reticulum calcium ATPase responsible for muscle relaxation, was upregulated, suggesting disrupted calcium homeostasis and contractile dysfunction linked to muscle fatigue and pain [21]. F9, coagulation factor IX, was also elevated. Beyond hemostasis, the coagulation cascade interacts closely with inflammation, and F9 is activated at tissue injury sites [22]. SLC6A4, a serotonin transporter that modulates pain signaling by serotonin reuptake, was increased in serum. Its upregulation suggests that mechanical loading may be associated with structural tissue damage and pain-related neurochemical pathways, consistent with clinical neck pain [23]. Taken together, these observations support MYH4, ATP2A1, F9, and SLC6A4 as potential injury-related biomarkers after 3-week centrifugation exposure.

The top 10 upregulated and 10 downregulated proteins following 4-week centrifugation were ETFB, CIAO2A, EML1, DCLK1, OSBPL1A, CAD, COL16A1, COG1, TSKU, ANTXR2; and INHBC, ACAT1, PEPD, LCN2, S100A8, MS4A1, SAR1B, CLU, GNB4, SAA3, respectively (**Figure 3D**). S100A8, a calprotectin subunit abundantly secreted by neutrophils and macrophages during chronic inflammation, acts as an endogenous alarm signal. Its elevated expression indicated that mechanical loading induced a sustained inflammatory microenvironment similar to that in degenerative disorders [24, 25]. Likewise, serum amyloid A3 (SAA3), an acute-phase protein, further verified persistent inflammation [26]. LCN2(lipocalin-2) is involved in innate immune responses and is induced by oxidative stress and inflammatory states, promoting chondrocyte apoptosis and osteoarthritis [27]. Increased MS4A1(CD20), a B lymphocyte marker, may be associated with specific immune activation in response to chronic disc injury [28]. INHBC, a TGF-β family member, was upregulated. As TGF-β is the most known pro fibrotic mediator, this indicates a possible link with enhanced profibrotic signaling, which may underlie fibrosis associated with chronic intervertebral disc degeneration [29]. Taken together, these data indicated S100A8, SAA3, LCN2, MS4A1, and INHBC as potential injury related biomarkers after 4-week centrifugation.

To further characterize the functional implications, Gene Ontology (GO) analysis was performed with the differentially expressed proteins from the 3-week group, with the top 10 enriched terms ranked by *p* value being selected for visualization in a bar plot (**Figure 3E**). In terms of Biological Process (BP), “the cellular response to sodium arsenite”, as well as

"response to sodium arsenite" and "hydrogen peroxide catabolic process", are significantly correlated with CAT. Sodium arsenite induces oxidative stress, and CAT functions as a core antioxidant enzyme that decomposes hydrogen peroxide, driving the enrichment of these terms. Separately, the response to salt involves ATP2A1, TRPC6, and SLC6A4, which regulate ion and osmotic homeostasis by controlling transmembrane ion fluxes. "Positive regulation of protein localization to the cell cortex" was mediated by EPB41L2 and RDX, cytoskeletal adaptors that maintain cell morphology and motility. In terms of molecular function (MF), "P-type ion transporter activity", "P-type transmembrane transporter activity", and "ATPase coupled monatomic cation transmembrane transporter activity" all refer to ATP2A1. As a P-type ATPase, ATP2A1 modulates intracellular calcium homeostasis by pumping Ca^{2+} into the sarcoplasmic reticulum, consistent with these functional annotations.

Gene Ontology (GO) analysis was conducted on the differentially expressed proteins between the 4-week centrifugation and control groups, with the top 10 enriched terms ranked by *p* value presented in **Figure 3F**. Enriched terms including "platelet degranulation" and "platelet alpha granule lumen" were associated with F9, SAA3, CLU, and LCN2. Platelet alpha granules store multiple inflammatory mediators and growth factors. F9 contributes to platelet activation, SAA3 can be secreted by platelets, and both CLU and LCN2 are stored in these granules. Their altered expression suggests sustained platelet activation under chronic injury, which amplifies inflammation and tissue remodeling via granule release. Terms related to "leukocyte chemotaxis", "myeloid leukocyte migration", and "granulocyte migration", were associated with S100A8, LCN2, SAA3, and INHBC. S100A8 is a potent neutrophil chemoattractant, while LCN2 and SAA3 also promote leukocyte recruitment. INHBC regulates inflammatory cell migration and activation. Additionally, S100A8 mediates oxidative stress by facilitating superoxide production via NADPH oxidase. Moreover, several proteins including SAA3, CLU, and APOD are associated with lipoprotein particles, such as high-density lipoproteins. During inflammation, SAA3 replaces ApoA1 on HDL and CLU exhibits apolipoprotein-like properties. These changes are potentially related to altered lipoprotein transport and dysregulated lipid metabolism secondary to chronic inflammation.

We then performed KEGG enrichment analysis on the differentially expressed proteins between the 3-week centrifugation and control groups. The top 15 enriched pathways ranked by *p*-value are displayed in a dot plot (**Figure 3G**). Notably, the "Efferocytosis" pathway was significantly enriched. Efferocytosis exerts a dual effect. Efficient efferocytosis promotes anti-inflammatory responses and tissue repair, whereas defective efferocytosis drives chronic inflammation. Its enrichment indicated that mechanical damage is potentially related to disc cell apoptosis and subsequent immune-mediated clearance. The "ECM-receptor interaction" pathway- a classic signature of intervertebral disc degeneration - was also enriched. As disc structure is highly dependent on extracellular matrix homeostasis, disruption of this pathway suggests impaired matrix architecture and altered cell-matrix crosstalk, likely mediated by receptors such as integrins. Additionally, the "Glutathione metabolism" pathway was enriched, consistent with the earlier differential expression of CAT. This further supports that mechanical loading induces oxidative stress, with cells activating antioxidant systems including glutathione metabolism to counteract injury. The "cAMP signaling pathway" was also significantly altered. As a central second messenger, cAMP regulates inflammation, apoptosis, and metabolic adaptation. Mechanical stimuli can influence cAMP dynamics, and pathway enrichment here suggests that mechanical injury may be associated with widespread reprogramming of intracellular signaling networks.

To further explore the biological implications of the proteomic changes, we conducted a KEGG pathway enrichment analysis on differentially expressed proteins identified between the 4-week centrifugation and control groups. The top 15 enriched pathways by *p*-value are displayed in a dot plot (**Figure 3H**). Among the enriched terms, "Proteoglycans in cancer" and "Glycosaminoglycan binding" were highly relevant, as they directly relate to intervertebral disc integrity. Proteoglycans, essential components of the nucleus pulposus, maintain tissue hydration and compressive resistance. Their sustained enrichment at the 4-week time point

was potentially related to ongoing matrix degradation and metabolic dysfunction. Though named for oncology, the "Proteoglycans in cancer" pathway reflects broader roles in regulating cell proliferation, adhesion, and migration-processes dysregulated in disc degeneration-with aberrant signaling potentially driving maladaptive tissue remodeling. The "ECM-receptor interaction" pathway, previously enriched at the 3-week group, was again enriched at 4-weeks, suggesting persistent disruption of cell-extracellular matrix communication and progressive matrix breakdown. "Peptidases and inhibitors" were also enriched, including matrix metalloproteinases and other proteases, reflecting the ongoing balance between tissue degradation and endogenous inhibition - a hallmark of chronic degeneration. Additionally, the "neutrophil extracellular trap (NET) formation" was enriched. NETs, released by neutrophils, exacerbate tissue damage and promote inflammation. Notably, this aligns with the earlier identification of S100A8, a known inducer of NET formation, further supporting a possible link with innate immune activation and disc pathology progression.

Candidate early warning and injury indicators in intervertebral disc proteomics of New Zealand rabbits

To explore additional candidate early cervical injury indicators, intervertebral disc samples from experimental and control animals were analyzed via proteomic techniques. PCA was performed on 32 samples, reducing multiple protein expression variables from high dimensions to a few independent variables. The first two principal components (PC) explained 33.3% of the total variation, with principal component 1 (PC1) accounting for 22.5% and principal component 2 (PC2) accounting for 10.8%. The results showed significant differences between sample groups and clear group separation (**Figure 4A**). Intersection analysis of differentially expressed proteins revealed that ECHS1 expression was altered by 1-4 weeks of centrifugation, while A0A5F9DDV3, G1SD41, RPL38, and RRAGB were dysregulated by 2-4 weeks of centrifugation (**Figure 4B**).

Compared with the control group, ECHS1 expression in centrifuged animals exhibited a distinct temporal pattern: initially downregulated in the first week, then significantly upregulated over the following three weeks. ECHS1 (short chain enoyl CoA hydrate 1) is a key enzyme in mitochondrial fatty acid beta oxidation, facilitating cellular energy production from lipids [30]. The nucleus pulposus cells, residing in an avascular, hypoxic microenvironment, mainly rely on anaerobic glycolysis for energy, with fatty acid oxidation as a critical auxiliary source. During disc degeneration, metabolic homeostasis and mitochondrial function are impaired. Altered ECHS1 expression may indicate metabolism reprogramming in response to mechanical injury, and biphasic pattern (initial downregulation followed by upregulation) may reflect dynamic changes from early/acute injury period to late/compensatory adaptation phase.

Compared with the control group, A0A5F9DDV3 and RRAGB were upregulated in centrifugation at 2, 3, and 4 weeks, while G1SD41 and RPL38 were downregulated. A0A5F9DDV3 (Collagen Type II Alpha 1 Chain) is the main structural protein in the extracellular matrix cartilage and nucleus pulposus, providing tissue tension and compressive strength [31]. RRAGB (Ras related GTP binding protein B) is a key regulatory factor of mTORC1 signaling pathway, a central signaling hub that enables cells to sense nutrient and energy status, regulating cell growth, synthesis metabolism, and autophagy. RRAGB modulates mTORC1 activity in response to amino acid availability [32]. Overactive mTORC1 inhibits autophagy, a degradative pathway essential for clearing damaged cellular components and preserving homeostasis under stress [33]. Notably, disruption of autophagic flux has been closely linked to intervertebral disc degeneration. In this context, altered RRAGB expression suggests that mechanical injury interferes with both disc cells upstream regulators and core signaling networks, potentially driving aberrant mTORC1 signaling, impairing autophagy, protein synthesis, and energy metabolism, and accelerating degenerative.

G1SD41 (lumican) showed significantly reduced expression. As a small leucine-rich proteoglycan, lumican is essential for collagen fiber assembly, diameter regulation, and tissue organization. By interacting with type II collagen and other matrix components, it helps preserve normal extracellular structure. Altered proteogly-

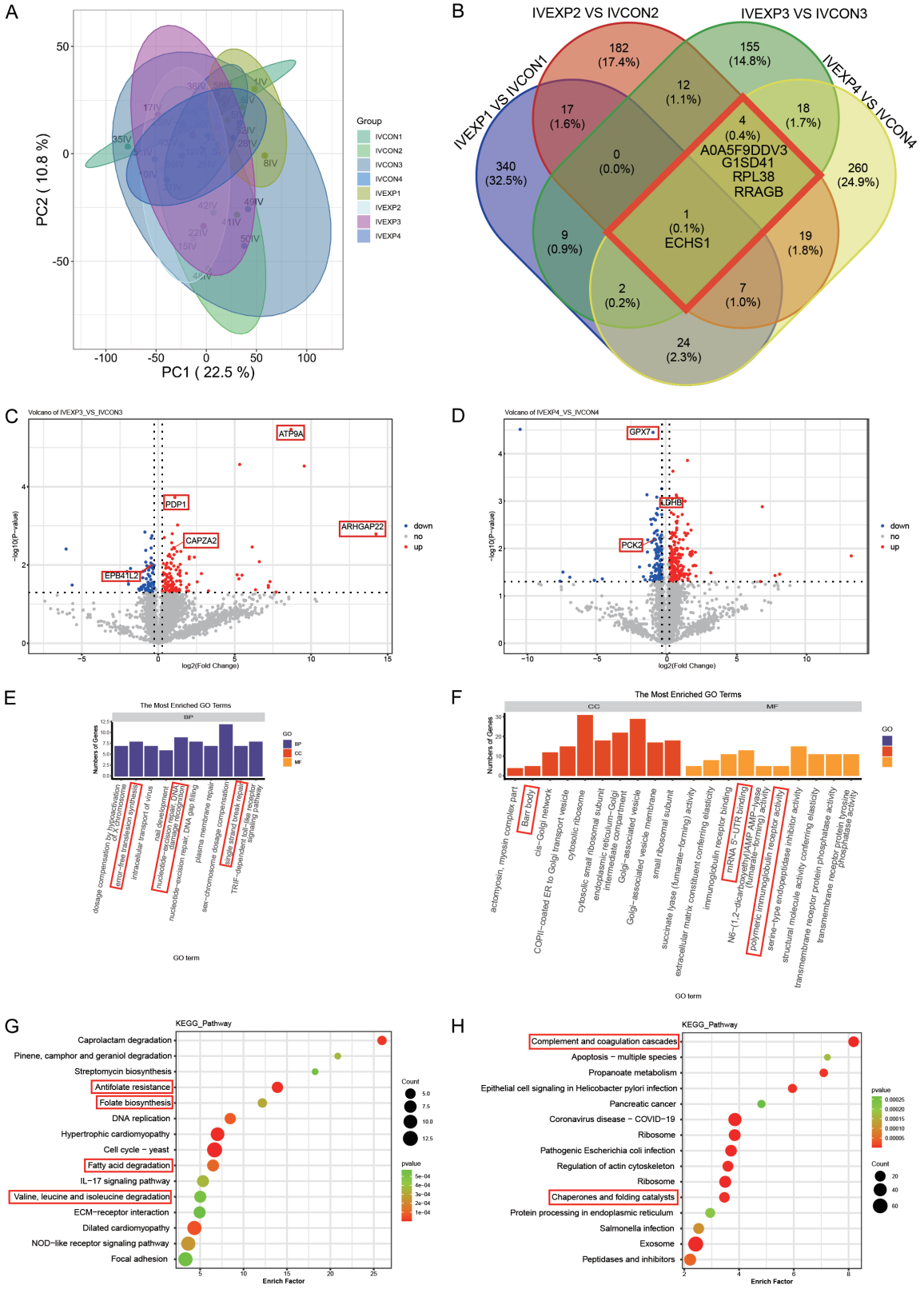

Figure 4. Proteomic analysis of cervical intervertebral disc tissue. A. Principal component analysis of proteins in experimental groups and control groups; B. Venn Differences and Similarities analysis of proteins in experimental groups and control groups, sample size (n=64); C. Volcano plot analysis of differentially expressed proteins in the 3-week experimental group compared with the 3-week control group; D. Volcano plot analysis of differentially

expressed proteins in the 4-week experimental group compared with the 4-week control group; E. GO analysis of differentially expressed proteins in the 3-week experimental group compared with the 3-week control group; F. GO analysis of differentially expressed proteins in the 4-week experimental group compared with the 4-week control group; G. KEGG analysis of differentially expressed proteins in the 3-week experimental group compared with the 3-week control group; H. KEGG analysis of differentially expressed proteins in the 4-week experimental group compared with the 4-week control group.

can expression has been previously reported in intervertebral disc degeneration, suggesting potential roles in modulating inflammatory and fibrotic responses [34]. Mechanical injury compromises extracellular matrix integrity, and reduced lumican levels may reflect impaired repair and reorganization of damaged collagen network.

Ribosomal Protein L38 (RPL38) was also found to be downregulated. As a direct marker of cellular biosynthetic activity [35], reduced RPL38 expression under cellular stress, including mechanical injury and oxidative stress, protein synthesis, may be associated with attenuated synthetic capacity in intervertebral disc cells, especially the nucleus pulposus following mechanical insult. This was further supported by concurrent changes in ECHS1 expression indicative of cellular energy deficiency.

We identified the top 10 most significantly downregulated and upregulated proteins after 3-weeks of centrifugation: NDC1, MTCH1, PLXDC2, MYOF, ESYT2, GAS2, SH3PXD2B, PTGFRN, EPB41L2, KIRREL1, PDP1, UBQLN4, KPNA1, VPS37B, SMC4, CAPZA2, SMCHD1, SNAPIN, ARHGAP22, ATP9A (**Figure 4C**). EPB41L2 (protein 4.1B), a downregulated membrane-cytoskeleton linker, is essential for preserving structural integrity. Its reduced expression in both tissue and serum samples from the 3-week centrifugation group suggested a possible link with impaired cellular mechanical stability and increased susceptibility [36]. In contrast, CAPZA2 (F-Actin Capping Protein Alpha-2 subunit) was upregulated. This protein regulates actin filament's length and dynamics. Dysregulated expression may impair actin cytoskeleton remodeling, compromising cell morphology and migratory ability [37]. Additionally, PDP1 (pyruvate dehydrogenase phosphatase 1) can activate pyruvate dehydrogenase, linking glycolysis to the tricarboxylic acid cycle [38].

The 10 most significantly downregulated and upregulated proteins after 4-weeks of centrifugation modeling were: ANKRD44, GPX7, AAK1, MRPL43, PCOLCE, P3H4, SHMT2, COPZ2, AIMP1, PCK2, SMCHD1, MYADM, LGALSL, LDHB, AASS, LGALS3, MROH7, KIF12, LSAMP and IGHM (**Figure 4D**). GPX7, PCK2, and LDHB are associated with oxidative stress and metabolic adaptation. GPX7 (Glutathione Peroxidase 7) is an endoplasmic reticulum associated antioxidant enzyme that scavenges peroxides and protects cells from endoplasmic reticulum stress [39]. PCK2 (Phosphoenolpyruvate Carboxykinase 2) is a key enzyme in mitochondrial gluconeogenesis that acts by converting oxaloacetate to phosphoenolpyruvate [40]. LDHB (Lactate Dehydrogenase B) catalyzes the interconversion of lactate and pyruvate, and plays an important role in the glycolysis process [41].

GO analysis was performed with the differential proteins between the 3-week centrifugation and control groups (**Figure 4E**). SMC4, SMCHD1, and KPNA1 were enriched in terms related to error-free translation synthesis, nucleotide-excision repair, single strand break repair. SMC4 is the core subunit of the lectin complex, regulating chromosome structure in DNA repair and replication. SMCHD1 is an epigenetic regulatory factor involved in DNA damage response and X chromosome inactivation. KPNA1 mediates nuclear-cytoplasmic transport and can transport DNA repair proteins into the nucleus. The enrichment of these proteins showed that the mechanical loading may be associated with significant DNA damage and epigenetic alterations, prompting active DNA repair mechanisms to maintain genomic stability.

Similar GO analysis was performed with the differential proteins between the 4-week centrifugation and control groups (**Figure 4F**). The Barr body is related to SMCHD1. Consistent with the 3-week group, SMCHD1 is a key regulatory factor for X chromosome inactivation and Barr body maintenance. Its re-emergence in the 4-week group may suggest sustained and severe epigenetic disorder. Immunoglobulin receptor binding and polymeric immunoglobulin receptor activity are associated with IGHM.

The polymeric immunoglobulin receptor facilitates the transcytosis of IgA and IgM, with I IgM acting as its ligand. The co-expression of these proteins may be associated with an active immune response and lymphocyte infiltration in degenerated intervertebral disc tissue.

Next, KEGG analysis was conducted with the differential proteins between the 3-week centrifugation and control groups (**Figure 4G**). Enrichment of fatty acid degradation and valine, leucine and isoleucine degradation indicated metabolic reprogramming. The nucleus pulposus cells mainly rely on anaerobic glycolysis. Under mechanical stress with increased energy demands, cells are forced to utilize alternative energy sources. The catabolism of fatty acids and branched chain amino acids could produce more ATP through β-oxidation and the tricarboxylic acid cycle. Folic acid and its derivatives (such as tetrahydrofolate) are the core component of one carbon metabolism, which is involved in purine and thymidine synthesis and crucial for DNA replication and repair. The enrichment of antiflate resistance and folate biosynthesis pathways may be associated with a significant increased nucleotides demand under stress conditions, likely to support damaged DNA repair.

KEGG analysis was also performed with the differential proteins between the 4-week centrifugation and control groups (**Figure 4H**). The complement and coagulation cascades pathway, a hallmark of chronic inflammation and immune dysregulation, was enriched. As the core component of innate immunity, complement system activation produces cytotoxic molecules that recruit and target cells; extensive crosstalk exists between the coagulation system and inflammation, with activated platelets releasing large amounts of inflammatory mediators. The enrichment of this pathway may be associated with chronic injury induced aberrant, persistent activation of the immune and coagulation systems, collectively exacerbating tissue damage. Ribosome, the primary site for protein synthesis, were significantly enriched, suggesting intervertebral disc cells were in a high synthetic state at 4 weeks. This may be potentially related to ECM synthesis/repair, inflammatory factors and antibody production to maintain immunity, and molecular chaperones synthesis to cope with stress. Moreover, the chaperones and folding catalysts pathway, closely related to endoplasmic reticulum protein processing, was also enriched. High protein synthesis can lead to endoplasmic reticulum stress. Molecular chaperones, such as heat shock proteins, assist in proper protein folding and prevents aggregation of misfolded proteins. Their upregulation may be associated with a cellular mechanism to preserve proteostasis under elevated protein synthesis pressure. Under combined chronic inflammation, oxidative stress, and endoplasmic reticulum stress, apoptosis represented an inevitable cellular outcome.

Discussion

This study was designed to determine the injury tolerance thresholds and candidate early molecular warning signals for horizontal acceleration induced cervical damage in New Zealand rabbits. Using imaging, histopathological assessment, and proteomic profiling, we quantitatively evaluated cervical responses to single and repeated acceleration exposures and identified serum and intervertebral disc tissue proteins as early injury indicators. Our findings reveal that the acute injury threshold were -5Gx for the trapezius muscle and -9Gx for the cervical intervertebral disc under single impact. In contrast, cumulative exposure to -6Gx for three weeks was sufficient to trigger intervertebral disc degeneration. Moreover, multi-omics analysis uncovered molecular network associated with progression tissue damage.

Our data revealed distinct injury thresholds: the trapezius muscle was injured at -5Gx, whereas the intervertebral disc showed structural damage at -9Gx. This marked difference underscores the inherent vulnerability of muscular tissue to acute horizontal loading, consistent with clinical observations that pilots frequently experience neck muscle stiffness and pain after exposure to high-G maneuvers [42]. Therefore, acute cervical symptoms appear to originate primarily from microtrauma within soft tissues, particularly the trapezius muscle, rather than from intervertebral disc damage. These findings highlight the need for enhanced dynamic support and energy-absorbing designs targeted at cervical musculature.

Beyond acute high-magnitude shocks, repeated low-intensity exposure also carries considerable risk. According to our findings, daily expo-

sure to -6Gx for three weeks results in detectable intervertebral disc degeneration on imaging and histopathology, emphasizing the pathogenic role of cumulative mechanical load. In contrast, the trapezius muscle showed no lasting pathological changes, likely due to its stronger regenerative capacity [43]. This difference highlights the high susceptibility of intervertebral discs to accumulated mechanical stress, partly due to their limited intrinsic repair capacity.

Using time-resolved proteomic profiling, we identified molecular signatures in serum and disc tissue that precede overt structural damage. Notably, four serum proteins, C1QTNF3 (A0A5F9CQH5), PSMA8, GPX6, and CAT, were significantly dysregulated as early as 1-2 weeks, well before imaging or histological changes were detectable. Their altered expression may be associated with coordinated early cellular response to sustained mechanical stress, including ECM remodeling, protein quality control, and antioxidant defenses. Taken together, these proteins may serve as promising blood-based biomarkers for early detection of cervical injury before clinical or radiological signs emerge.

During the later injury phase (weeks 3-4), the molecular landscape became more complex. Increased S100A8 and IGHM indicate chronic inflammation and adaptive immunity activation, while altered SLC6A4 and DCLK1 suggested pain-related neural sensitization. Additionally, upregulated COL16A1 and INHBC reflected pathological fibrosis and aberrant matrix remodeling. These observations suggested that our model recapitulates the core pathological features of clinical disc degeneration and reveals potential therapeutic targets for modulating inflammation, immunity, and neural invasion.

Methodologically, this work introduces several advances. We designed a custom impact device that accurately simulates horizontal inertial forces with high controllability and efficiency, providing a useful platform for biomechanical research. We also established a reproducible chronic injury model using cumulative acceleration exposures in an animal centrifuge, mimicking long-term mechanical loading. The New Zealand rabbits were selected for their cervical spine anatomy and biomechanical similarity to humans [44], supporting translational relevance. However, interspecies differences must be considered, and direct extrapolation to humans requires caution. Further validation in larger animal or clinical cohorts is needed.

Several limitations of this study should be acknowledged. First, we did not perform functional behavioral assessments, such as evaluating pain or mobility, limiting correlations between clinical phenotypes and the molecular changes. Second, although sufficient for exploratory analysis, the sample size was relatively small. Larger cohorts are required to validate the reliability and generalizability of the identified biomarkers. Furthermore, these candidate markers have not been verified in independent animal groups or human pilots, necessitating further validation prior to clinical translation.

Given the above findings and limitations, several directions warrant further investigation. First, integrating functional imaging with behavioral assessments may enable a more comprehensive evaluation framework covering structural, molecular changes and functional alterations. Second, the candidate early-warning biomarkers identified here require validation in larger independent cohorts to assess their sensitivity and specificity more rigorously. Finally, informed by the pathway analyses particularly those involving oxidative stress and inflammation, future studies may explore whether targeted interventions such as pharmacological agents or rehabilitative strategies can alleviate or reverse acceleration-induced cervical injury.

In summary, using the New Zealand rabbits model, this study determined acute and chronic injury thresholds for cervical damage induced by horizontal acceleration. Through multi-omics analysis, we delineated the dynamic molecular landscape that charts the progression from early stress responses to established degenerative pathology. These findings may help elucidate the mechanisms underlying pilot neck injury, which could offer key experimental evidence, and might provide a molecular framework to support the development of early monitoring tools and targeted protective strategies.

Disclosure of conflict of interest

None.

Address correspondence to: Dr. Wei Wang, Naval Medical Center of The People's Liberation Army, Navy Medical University, No. 880 Xiangyin Road, Yangpu District, Shanghai 200082, The People's Republic of China. E-mail: wwang_fd@fudan.edu.cn

References

[1] Zhu F, Voo L, Balakrishnan K, Lapera M and Cheng Z. Numerical analysis of pilot neck injury risk during high-g maneuvers in air combat. Int J Numer Method Biomed Eng 2025; 41: e70022

[2] Green ND. Acute soft tissue neck injury from unexpected acceleration. Aviat Space Environ Med 2003; 74: 1085-1090.

[3] Verde P, Trivelloni P, Angelino G, Morgagni F and Tomao E. Neck pain in F-16 vs. Typhoon fighter pilots. Aerosp Med Hum Perform 2015; 86: 402-406.

[4] Keskimölö T, Pernu J, Karppinen J, Niinimäki J, Oura P, Leino T and Honkanen T. Degenerative cervical spine changes among early career fighter pilots: a 5-year follow-up. BMJ Mil Health 2023; 169: 291-296.

[5] Vallejo Desviat P, Esteban Benavides B, López López JA, Rios-Tejada F, Bárcena A, Alvarez-Sala F and Alonso Rodríguez C. Surgical correction of disc pathology in fighter pilots: a review of 14 cases. Aviat Space Environ Med 2007; 78: 784-788.

[6] Lang RW, Porensky P and Fraser JJ. Burden and risk factors of cervical spine conditions in military aircrew from 1997 to 2015: a retrospective cohort study. Mil Med 2025; 190: e766-e776.

[7] Li ZH, Li SP, Li YH, Wang YC, Tang ZY, Xu KY, Li XR, Tan Z, Pan JY, Liu JT, Jiang H, Ma ZJ, Dai YX and Yu PF. Identification of aging-related biomarkers for intervertebral disc degeneration in whole blood samples based on bioinformatics and machine learning. Front Immunol 2025; 16: 1565945.

[8] Harinathan B, Jebaseelan D, Yoganandan N and Vedantam A. Effect of cervical stenosis and rate of impact on risk of spinal cord injury during whiplash injury. Spine (Phila Pa 1976) 2023; 48: 1208-1215.

[9] Zheng Z, Chen J, Xu J, Jiang B, Li L, Li Y, Dai Y and Wang B. Peripheral blood RNA biomarkers can predict lesion severity in degenerative cervical myelopathy. Neural Regen Res 2025; 20: 1764-1775.

[10] Xia LZ, Zheng YP, Xu HG and Liu P. Effect of anterior cervical discectomy and fusion on adjacent segments in rabbits. Int J Clin Exp Med 2014; 7: 4291-4299.

[11] Zhu XR, Deng TZ, Pang JL, Liu B and Ke J. Effect of high positive acceleration (plus Gz) environment on dental implant osseointegration: a preliminary animal study. Biomed Environ Sci 2019; 32: 687-698.

[12] Longuespée R, Casadonte R, Schwamborn K, Reuss D, Kazdal D, Kriegsmann K, von Deimling A, Weichert W, Schirmacher P, Kriegsmann J and Kriegsmann M. Proteomics in pathology. Proteomics 2018; 18: 1700361.

[13] Ozkadif S and Eken E. Craniometric measurements of New Zealand rabbits skull from three-dimensional reconstruction images. ARC Journal of Animal and Veterinary Sciences 2016; 2: 2455-2518.

[14] Chen B, Ding J, Zhao Z, Jin J, Zhu S, Zang M, Xue B and Liu Y. Mechanical loading improves engineered tendon formation with muscle-derived cells: an in vivo analysis. Plast Reconstr Surg 2018; 142: 685E-693E.

[15] Ke W, Xu H, Zhang C, Liao Z, Liang H, Tong B, Yuan F, Wang K, Hua W, Wang B and Yang C. An overview of mechanical microenvironment and mechanotransduction in intervertebral disc degeneration. Exp Mol Med 2025; 57: 2157-2168.

[16] Schanbacher C, Hermanns HM, Lorenz K, Wajant H and Lang I. Complement 1q/tumor necrosis factor-related proteins (CTRPs): structure, receptors and signaling. Biomedicines 2023; 11: 559.

[17] Zhu Y, Shigeyoshi K, Hayakawa Y, Fujiwara S, Kishida M, Ohki H, Horibe T, Shionyu M, Mizukami T and Hasegawa M. Acceleration of protein degradation by 20s proteasome-binding peptides generated by in vitro artificial evolution. Int J Mol Sci 2023; 24: 17486.

[18] Brigelius-Flohé R and Maiorino M. Glutathione peroxidases. Biochim Biophys Acta 2013; 1830: 3289-3303.

[19] Jin LY, Lv ZD, Wang K, Qian L, Song XX, Li XF and Shen HX. Estradiol alleviates intervertebral disc degeneration through modulating the antioxidant enzymes and inhibiting autophagy in the model of menopause rats. Oxid Med Cell Longev 2018; 2018: 7890291.

[20] Weiss A and Leinwand LA. The mammalian myosin heavy chain gene family. Annu Rev Cell Dev Biol 1996; 12: 417-439.

[21] Jin S, Kim J, Willert T, Klein-Rodewald T, Garcia-Dominguez M, Mosqueira M, Fink R, Esposito I, Hofbauer LC, Charnay P and Kieslinger M. Ebf factors and MyoD cooperate to regulate muscle relaxation via Atp2a1. Nat Commun 2014; 5: 3793.

[22] Lowe GD. Factor IX and thrombosis. Br J Haematol 2001; 115: 507-513.

[23] Huang C, van Wijnen AJ and Im HJ. Serotonin Transporter (5-Hydroxytryptamine Transporter,

SERT, SLC6A4) and Sodium-dependent reuptake inhibitors as modulators of pain behaviors and analgesic responses. J Pain 2024; 25: 618-631.
[24] Geven EJ, van den Bosch MH, Di Ceglie I, Ascone G, Abdollahi-Roodsaz S, Sloetjes AW, Hermann S, Schäfers M, van de Loo FA, van der Kraan PM, Koenders MI, Foell D, Roth J, Vogl T and van Lent PL. S100A8/A9, a potent serum and molecular imaging biomarker for synovial inflammation and joint destruction in seronegative experimental arthritis. Arthritis Res Ther 2016; 18: 247.
[25] Schelbergen RF, de Munter W, van den Bosch MH, Lafeber FP, Sloetjes A, Vogl T, Roth J, van den Berg WB, van der Kraan PM, Blom AB and van Lent PL. Alarmins S100A8/S100A9 aggravate osteophyte formation in experimental osteoarthritis and predict osteophyte progression in early human symptomatic osteoarthritis. Ann Rheum Dis 2016; 75: 218-225.
[26] den Hartigh LJ, Wang S, Goodspeed L, Ding Y, Averill M, Subramanian S, Wietecha T, O'Brien KD and Chait A. Deletion of serum amyloid A3 improves high fat high sucrose diet-induced adipose tissue inflammation and hyperlipidemia in female mice. PLoS One 2014; 9: e108564.
[27] Villalvilla A, García-Martín A, Largo R, Gualillo O, Herrero-Beaumont G and Gómez R. The adipokine lipocalin-2 in the context of the osteoarthritic osteochondral junction. Sci Rep 2016; 6: 29243.
[28] Mattiola I, Mantovani A and Locati M. Feature review the tetraspan MS4A family in homeostasis, immunity, and disease. Trends Immunol 2021; 42: 764-781.
[29] Sun T, Huang Z, Liang WC, Yin J, Lin WY, Wu J, Vernes JM, Lutman J, Caplazi P, Jeet S, Wong T, Wong M, DePianto DJ, Morshead KB, Sun KH, Modrusan Z, Vander Heiden JA, Abbas AR, Zhang H, Xu M, N'Diaye EN, Roose-Girma M, Wolters PJ, Yadav R, Sukumaran S, Ghilardi N, Corpuz R, Emson C, Meng YG, Ramalingam TR, Lupardus P, Brightbill HD, Seshasayee D, Wu Y and Arron JR. TGFβ2 and TGFβ3 isoforms drive fibrotic disease pathogenesis. Sci Transl Med 2021; 13: eabe0407.
[30] Fu Q, Qiu R, Li S, Qin Y, Lu Z, Liyao S, Yang Z, Cheng X, Chen Y, Xu H and Cheng Y. ECHS1: pathogenic mechanisms, experimental models, and emerging therapeutic strategies. Orphanet J Rare Dis 2025; 20: 430.
[31] Wang X, Sun J, Tan J, Fang P, Chen J, Yuan W, Chen H and Liu Y. Effect of sIL-13Rα2-Fc on the progression of rat tail intervertebral disc degeneration. J Orthop Surg Res 2019; 14: 386.
[32] Carlin MB, Tanner RE, Agergaard J, Jalili T, McClain DA and Drummond MJ. Skeletal muscle Ras-related GTP binding B mRNA and protein expression is increased after essential amino acid ingestion in healthy humans. J Nutr 2014; 144: 1409-1414.
[33] Han X, Goh KY, Lee WX, Choy SM and Tang HW. The importance of mTORC1-autophagy axis for skeletal muscle diseases. Int J Mol Sci 2022; 24: 297.
[34] Li Z, Sun C, Chen M and Wang B. Lumican silencing alleviates tumor necrosis factor-α-induced nucleus pulposus cell inflammation and senescence by inhibiting apoptosis signal regulating kinase 1/p38 signaling pathway via inactivating Fas ligand expression. Bioengineered 2021; 12: 6891-6901.
[35] Fang Y, Zhang F, Zhao F, Wang J, Cheng X, Ye F, He J, Zhao L and Su Y. RpL38 modulates germ cell differentiation by controlling Bam expression in Drosophila testis. Sci China Life Sci 2024; 67: 2411-2425.
[36] Wang T, Ding G, Wang X, Cui Y, Ma X, Ma J and Wu J. Expression of EPB41L2 in cancer-associated fibroblasts: prognostic implications for bladder cancer and response to immunotherapy. Arch Med Res 2024; 55: 102927.
[37] Ohishi T, Yoshida H, Katori M, Migita T, Muramatsu Y, Miyake M, Ishikawa Y, Saiura A, Iemura SI, Natsume T and Seimiya H. Tankyrase-binding protein TNKS1BP1 regulates actin cytoskeleton rearrangement and cancer cell invasion. Cancer Res 2017; 77: 2328-2338.
[38] Li Y, Shen J, Cheng CS, Gao H, Zhao J and Chen L. Overexpression of pyruvate dehydrogenase phosphatase 1 promotes the progression of pancreatic adenocarcinoma by regulating energy-related AMPK/mTOR signaling. Cell Biosci 2020; 10: 95.
[39] Kim HJ, Lee Y, Fang S, Kim W, Kim HJ and Kim JW. GPx7 ameliorates non-alcoholic steatohepatitis by regulating oxidative stress. BMB Rep 2020; 53: 317-322.
[40] Zhang J, He W, Liu D, Zhang W, Qin H, Zhang S, Cheng A, Li Q and Wang F. Phosphoenolpyruvate carboxykinase 2-mediated metabolism promotes lung tumorigenesis by inhibiting mitochondrial-associated apoptotic cell death. Front Pharmacol 2024; 15: 1434988.
[41] Ye Y, Yang F, Gu Z, Li W, Yuan Y, Liu S, Zhou L, Han B, Zheng R and Cao Z. Fibroblast growth factor pathway promotes glycolysis by activating LDHA and suppressing LDHB in a STAT1-dependent manner in prostate cancer. J Transl Med 2024; 22: 474.
[42] Moon BJ, Choi KH, Yun C and Ha Y. Cross-sectional study of neck pain and cervical sagittal alignment in air force pilots. Aerosp Med Hum Perform 2015; 86: 445-451.

[43] Roman W, Pinheiro H, Pimentel MR, Segalés J, Oliveira LM, García-Domínguez E, Gómez-Cabrera MC, Serrano AL, Gomes ER and Muñoz-Cánoves P. Muscle repair after physiological damage relies on nuclear migration for cellular reconstruction. Science 2021; 374: 355-359.

[44] Kong MH, Do DH, Miyazaki M, Wei F, Yoon SH and Wang JC. Rabbit model for in vivo study of intervertebral disc degeneration and regeneration. J Korean Neurosurg Soc 2008; 44: 327-333.

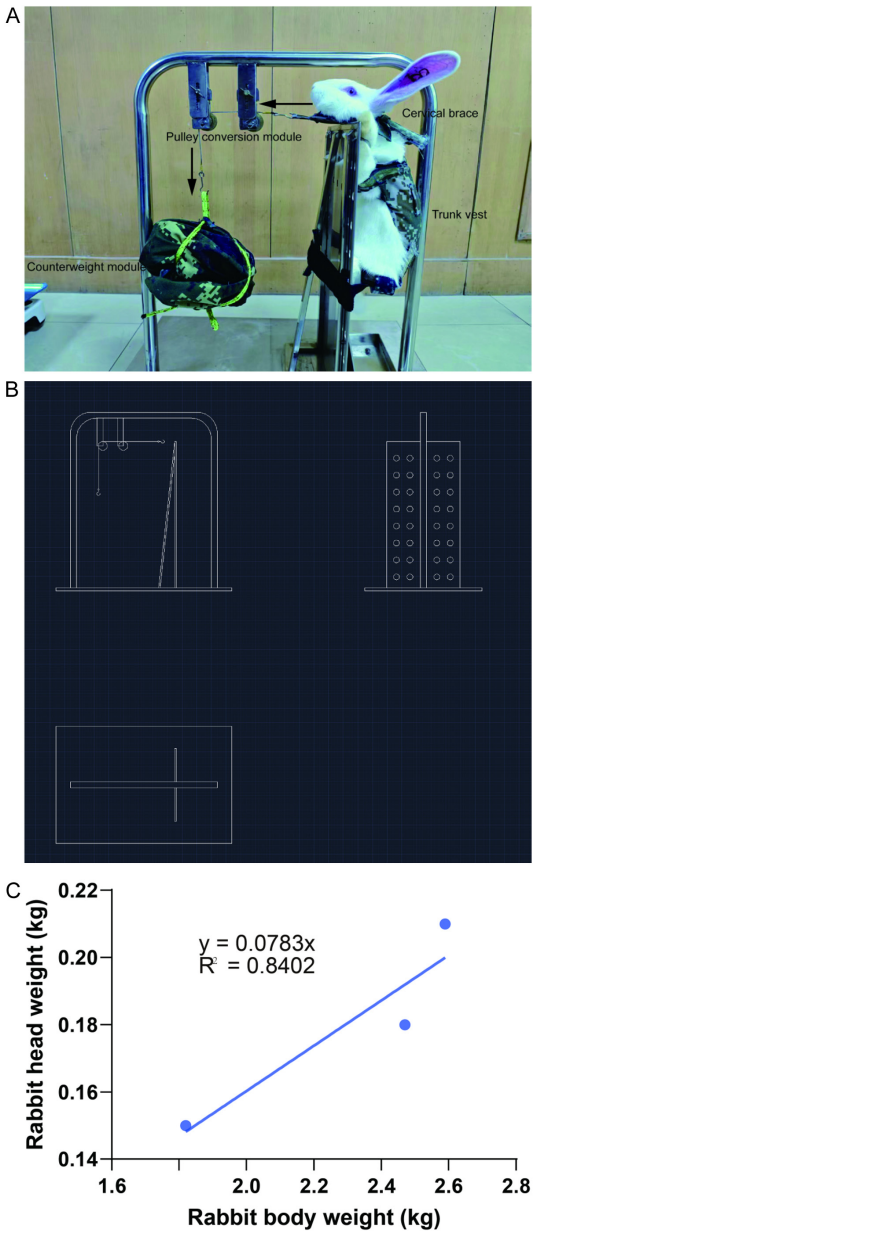

Figure S1. A. Real picture of the single-impact device; The arrow direction indicates the force direction; B. CAD drawing of the single-impact device; C. The relationship between the body weight and head weight of rabbits. This relationship is derived from a pre-experiment with n=3 animals, and is intended only for estimation of head weight.

Table S1. Measurement values of body weight and head weight of New Zealand rabbits

Rabbit ID	Rabbit body weight (kg)	Rabbit head weight (kg)
Pre 1	2.59	0.21
Pre 2	2.47	0.18
Pre 3	1.82	0.15

Table S2. The experimental details regarding Cervical -Gx overload

Grouping	Animal ID	Body Weight (g)	Head Weight (g)	Counterweight (g)
-5Gx	81	3180	248	1250
-5Gx	82	3230	253	1265
-5Gx	83	3100	243	1215
-7Gx	84	2970	233	1631
-7Gx	85	3330	261	1827
-7Gx	86	2410	189	1323
-9Gx	87	3000	235	2115
-9Gx	88	2650	207	1863
-9Gx	89	3240	254	2286
-11Gx	90	3190	250	2750
-11Gx	91	2660	208	2288
-11Gx	92	2640	207	2277
-13Gx	93	2660	208	2704
-13Gx	94	2540	199	2587
-13Gx	95	2590	203	2639
-15Gx	96	2660	208	3120
-15Gx	97	2790	218	3270
-15Gx	98	2450	192	2880

A

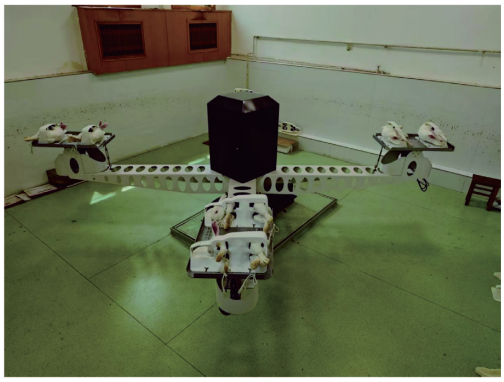

B

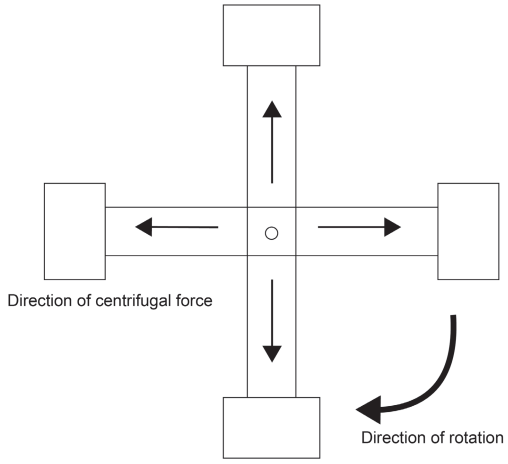

C

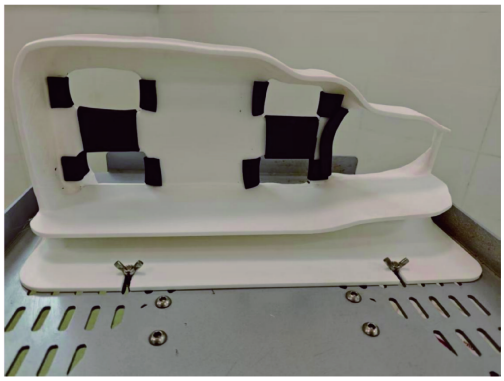

D

Radius	2 meter
Acceleration range	-1Gx to-16Gx
Loading protocol	-6Gx × 1min 5 minute interval 5 times per day

Figure S2. A. Real picture of the centrifugation system; B. Schematic of the centrifugation system; The straight arrow indicates the direction of centrifugal force, while the curved arrow indicates the direction of rotation of the centrifuge; C. Rabbit fixation/constraint design; D. Key parameters of the centrifugation system.